Research on Parameter Identification Algorithm of Permanent Magnet Synchronous Motor Considering Dead Time Compensation

Chengmin Wang* **and Aiyuan Wang**

Abstract—A parameter identification method based on an improved hunter prey algorithm is proposed to address the issues of poor accuracy and speed in traditional permanent magnet synchronous motor parameter identification methods. By using the Fuch infinite folding chaotic strategy to evenly distribute the initial individuals to enrich their diversity and using the golden sine algorithm to optimize the population search path, the algorithm's local development ability and global search ability are improved. The reasons for the dead time effect of the inverter are analyzed, and the input voltage is compensated for through the rotation coordinate method. SIMULINK simulation and physical experiment indicate that the improved algorithm has faster rate of convergence and higher recognition accuracy than the unmodified algorithm, and can effectively identify motor parameters. On this basis, adding dead time compensation effectively eliminates partial harmonics of the phase current and suppresses the occurrence of zero current clamping phenomenon. Compared with the situation without dead time compensation, the identification error of the four parameters has decreased from below 4.23% to below 2.21%.

1. INTRODUCTION

Compared to traditional electric excitation synchronous motors and asynchronous motors, permanent magnet synchronous motors (PMSMs) have higher operating efficiency and power density. In addition, PMSM also has the characteristics of small size and reliable structure, and is widely used in electric vehicles, industrial robots, aerospace satellites, variable frequency compressors, energy-saving household appliances, and other fields [1, 2]. In order to achieve good control performance of PMSM, it is necessary to obtain the electrical parameters of the motor in real-time. Affected by factors such as motor temperature rise and magnetic circuit saturation, the stator resistance, rotor permanent magnet flux, and stator inductance of PMSM change in real-time. If the temperature rise increases the stator resistance, it increases the copper loss of the motor. The eddy current loss in the permanent magnet intensifies the heating of the permanent magnet and reduces the amplitude of the rotor permanent magnet flux and the electromagnetic torque output, leading to permanent loss of excitation of the rotor permanent magnet. In addition, due to the saturation and cross saturation effects of the motor magnetic circuit, the stator inductance value decreases with the increase of current. The changes in PMSM parameters reflect the changes in motor faults, operating efficiency, and other performance. Real time and accurate acquisition of motor parameters is of great significance for tuning regulator parameters and achieving precise motor control.

The mathematical model of PMSM in synchronous rotating coordinate system is an equation with rank 2, and the motor has four electrical parameters, which are stator resistance, rotor permanent magnet flux, d-axis inductance, and q-axis inductance. According to system identification theory, if the number of parameters to be identified is more than the rank of the model, the identification equation will be in an under-rank state [3], and the identification parameters cannot converge to the correct

value, resulting in obvious errors. Presently, many scholars use various intelligent algorithms and other mathematical optimization strategies to solve underrank problems [4–6]. There are two main solutions to the underrank problem of the model equation for online identification of PMSM parameters. One is to reduce the number of parameters to be identified, and the other is to increase the rank of the model equation.

Reducing the number of parameters to be tested involves setting one to two parameters as constant values and identifying the remaining parameters online [7]. By reducing the number of parameters to be identified, a full rank equation is constructed, while fixed parameters may change during motor operation. By constructing a full rank equation with a fixed portion of motor parameters, the impact of parameter changes on identification accuracy during motor operation is essentially not eliminated, leading to local convergence or divergence of identification results.

Scholars have also conducted research on increasing the number of model equations to solve the problem of low rank. On the one hand, by measuring additional electrical signals, an equation containing the parameters to be identified is constructed, increasing the rank of identification equations for permanent magnet synchronous motors by injecting AC disturbance current into the direct axis under steady-state operating conditions, but does not consider the influence of motor magnetic saturation. The adaptive inertia weight particle swarm optimization algorithm based on the logistic function is used in [8] to realize the online identification of PMSM electrical and mechanical parameters by injecting current pulses into the straight axis. The stator resistance and rotor permanent magnet flux are identified in [9] by injecting three-level step angle pulses into the system. However, this method is still based on the nonlinear compensation strategy of the inverter and without considering the changes in inductance caused by injection angle pulses, which inevitably leads to overcompensation or undercompensation. The voltage model of PMSM in the AC and DC coordinate systems is utilized in [10] to inject disturbance current into the direct axis and use two time dimension affine projection algorithms (APA) to achieve simultaneous identification of stator resistance, stator inductance, and rotor permanent magnet flux. References [11–13] adopt slope and sine flux linkage to identify both stator and rotor resistances in a sensorless control system for asynchronous motors. In [14], an adaptive observer with strict stability parameters for speed and rotor resistance is established, proving that global stability of speed identification can be achieved in sensorless drive systems of asynchronous motors. Reference [15] adopts the information provided by harmonic back electromotive force (HBEMF) to construct an identification equation, which eliminates the need to inject additional disturbance signals and allows for the identification of an additional parameter.

Currently, frequency conversion control for most of the PMSMs is achieved through the use of inverters. However, inverter is not an ideal switching device. It has dead time, delay time of switching on and off, saturation voltage drop of switching tube, and conduction voltage drop of body diode, which may contribute to voltage error. The voltage applied to the motor is a Pulse Width Modulation (PWM) pulse output by the inverter, and it is difficult to obtain the actual phase voltage value applied to the motor without introducing the neutral point of the motor. Reference [16] established an accurate disturbance voltage estimation model, which includes current harmonics and their derivatives. Through experiments, the authors obtained a conclusion that the derivative of d-axis current harmonics plays a major role in the estimation error of disturbance voltage. On this basis, two methods were proposed to reduce the estimation error of disturbance voltage, thereby improving the accuracy of motor parameter identification. The treatment of inverter nonlinearity is still mainly based on various forms of inverter nonlinear compensation, which are divided into time compensation method and voltage compensation method. Most methods based on time compensation only consider the impact of dead time. The time compensation method is to adjust the width of the driving pulse signal of the inverter power transistor according to the magnitude of the error voltage and the polarity of the three-phase stator current of the motor, achieving dead time compensation. This method also uses the polarity of the current as the basis for the time compensation amount. Presently, nonlinear compensation for inverters is mostly based on voltage compensation method. Reference [17] designs a convenient phase voltage measurement circuit jumping out of the idea of nonlinear compensation for inverters. The circuit is mainly composed of a voltage divider and a low-pass filter, to detect three-phase PWM pulse voltage in real time, replacing the instruction voltage output by the controller, while this method still requires compensation for phase shift and amplitude attenuation caused by hardware low-pass filter. Reference [18] analyzes

the influence of distortion voltage caused by Voltage Source Inverter (VSI) nonlinearity on parameter identification, and experimental results show that the q-axis inductance can be accurately identified even without correcting the distortion voltage. It is also proposed that the compensation for distorted voltage can improve the accuracy of motor parameter identification when the motor is running at low speed. Reference [19] adopts extended Kalman filter (EKF) to estimate distortion voltage, resistance and flux linkage in real time, which can compensate distortion voltage in real time. The results show that the identification accuracy of resistance and flux linkage is better, but the fifth order identification model uses the first order Taylor series, which has poor dynamic performance. Reference [20] proposes a parameter identification method for dynamic learning particle swarm optimization (PSO), which simultaneously identifies distorted voltage and electrical parameters, improving identification accuracy. However, the design process of this method is complex, and its dynamic performance has not been verified. Reference [21] proposes a model predictive control method for permanent magnet synchronous motor based on parameter identification and dead time compensation. The harmonic components in the current are quickly filtered by adaptive linearity (ADALINE) method and recursive least square (RLS) algorithm, and the dead time compensation control is completed. It is proved that this method can effectively suppress steady-state current errors, improve current control performance, and accelerate the dynamic response of speed by experiments.

In this paper, a parameter identification method for permanent magnet synchronous motors considering dead time compensation is proposed. In response to the dead time effect of voltage source inverters, the rotating coordinate method is used to compensate the input voltage of the identification algorithm. By improving the algorithm, the motor resistance, permanent magnet flux, and inductance parameters of the d-q axis are identified.

This article consists of five sections. In Section 2, the mathematical model of permanent magnet synchronous motor and the dead time effect and compensation method of inverter are mainly introduced. In Section 3, the principle of parameter identification based on dead zone compensation and permanent magnet synchronous motor vector control is mainly introduced. In Section 4, the algorithm is evaluated using a benchmark function, and its effectiveness and superiority are verified through Matlab/Simulink simulation. The identification results before and after adding dead zone compensation are compared through an experimental platform. In Section 5, the research content and achievements of this article are summarized.

2. PMSM MATHEMATICAL MODEL AND INVERTER DEAD TIME EFFECT

2.1. PMSM Mathematical Model

Based on ignoring the eddy current loss and iron loss of PMSM, the stator voltage equation of PMSM in a synchronous rotating coordinate system is obtained, as shown in Equation (1):

$$\begin{cases} \dfrac{di_d}{dt} = -\dfrac{R_s}{L_d}i_d + \dfrac{L_q}{L_d}\omega_e i_q + \dfrac{u_d}{L_d} \\ \dfrac{di_q}{dt} = -\dfrac{R_s}{L_q} - \dfrac{L_d}{L_q}\omega_e i_d + \dfrac{u_q}{L_q} - \dfrac{\psi_f}{L_q}\omega_e \end{cases} \tag{1}$$

where u_d, u_q, i_d, i_q, L_d, L_q are the voltage, current, and inductance of the d and q axes, respectively; R_s is the stator resistance; ψ_f is the permanent magnet magnetic chain; ω_e is the electrical angular velocity of the rotor.

Based on the vector control strategy, when the motor operates stably, it is approximately assumed that:

$$\begin{cases} \dfrac{di_d}{dt} = 0 \\ \dfrac{di_q}{dt} = 0 \end{cases} \tag{2}$$

Under the control strategy of $i_d = 0$, the PMSM discrete voltage equation in the synchronous rotating coordinate system is obtained:

$$\begin{cases} u_d(k) = -\omega_e(k)L_q i_q(k) \\ u_q(k) = R_s i_q(k) + \psi_f \omega_e(k) \end{cases} \tag{3}$$

It is not difficult to see from the equation that the four unknown parameters of the equation system have countless solutions. One of the strategies commonly adopted by most intelligent identification methods nowadays is to inject negative sequence weak magnetic current into the stator d-axis. Under the condition of injecting weak magnetic current into the stator d-axis, the data sampling method is shown in Figure 1.
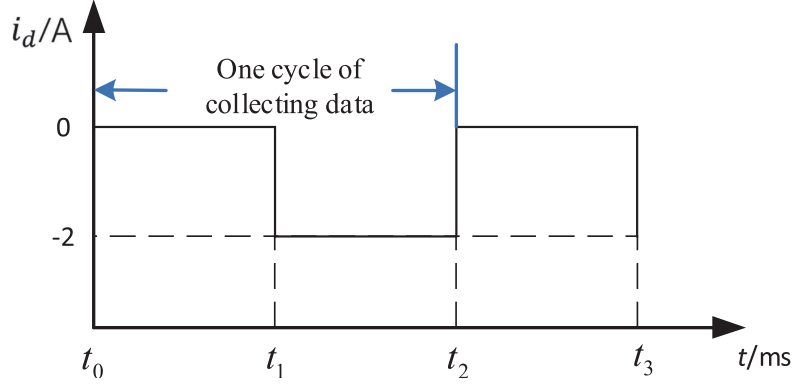

Figure 1. The diagram of data sampling.

Collect data from two strategies within one cycle to form a full rank equation system, as shown in Equation (4):

$$\begin{cases} u_{d0}(k_0) = -\omega_{e0}(k_0)L_q i_{q0}(k_0) \\ u_{q0}(k_0) = R_s i_{q0}(k_0) + \psi_f \omega_{e0}(k_0) \\ u_{d1}(k_1) = R_s i_{d1}(k_1) - L_q \omega_{e1}(k_1) i_{q1}(k_1) \\ u_{q1}(k_1) = R_s i_{q1}(k_1) + \psi_f \omega_{e1}(k_1) + L_d \omega_{e1}(k_1) i_{d1}(k_1) \end{cases} \tag{4}$$

where $u_{d0}(k_0)$, $u_{q0}(k_0)$, $i_{q0}(k_0)$, $\omega_{e0}(k_0)$ are the k-th sampling data during the t_0-t_1 time in Figure 1; $u_{d1}(k_1)$, $u_{q1}(k_1)$, $i_{d1}(k_1)$, $i_{q1}(k_1)$, $\omega_{e1}(k_1)$ are the k-th sampling data within the t_1-t_2 time in Figure 1.

2.2. Inverter Dead-Time Effect and Compensation

For voltage source inverter circuit, two switching devices on the same bridge arm cannot be turned on at the same time. Therefore, the introduction of dead time and the delay time of switching on or off will lead to the existence of nonlinear characteristics of the inverter. The output voltage error caused by the dead time effect of the inverter [22] is shown in Equation (5):

$$\Delta V = \frac{t_d + t_{on} + t_{off}}{T_S}(V_{dc} - V_{sat} + V_d) + \frac{V_{sat} + V_d}{2} \tag{5}$$

where t_d is the dead time; t_{on} and t_{off} are the delay times for opening and closing thyristors, respectively; T_S is the period of PWM pulse modulation; V_{dc} is the DC bus voltage; V_d is the forward voltage drop of the diode; V_{sat} is the saturation voltage drop of the switch;

The relationship between the reference voltage and the actual output voltage of PMSM [23] is shown in Equation (6) and Equation (7):

$$\begin{bmatrix} u_{d.real} \\ u_{q.real} \end{bmatrix} = \begin{bmatrix} u_{d.ref} \\ u_{q.ref} \end{bmatrix} - \Delta V \begin{bmatrix} D_d \\ D_q \end{bmatrix} \tag{6}$$

$$\begin{bmatrix} D_d \\ D_q \end{bmatrix} = \sqrt{\frac{2}{3}} \begin{bmatrix} \cos\theta & \cos\left(\theta - \frac{2}{3}\pi\right) & \cos\left(\theta + \frac{2}{3}\pi\right) \\ -\sin\theta & -\sin\left(\theta - \frac{2}{3}\pi\right) & -\sin\left(\theta + \frac{2}{3}\pi\right) \end{bmatrix} \begin{bmatrix} \text{sgn}(i_u) \\ \text{sgn}(i_v) \\ \text{sgn}(i_w) \end{bmatrix} \tag{7}$$

where D_d and D_q are the compensation components under the d-q axis system, respectively.

3. FG-HPO ALGORITHM

3.1. Hunter Prey Optimization Algorithm

Hunter prey optimization algorithm is a new swarm intelligence optimization algorithm proposed by Naruei et al. in 2022 [24]. The authors are inspired by hunters attacking individuals far away from the prey population and constantly adjusting their position based on the average population position of the prey. At the same time, the prey will constantly adjust its position to incline itself towards a safer location.

1) Initialize population members
   Set them to $(\vec{x}) = \{\vec{x}_1, \vec{x}_2, \ldots, \vec{x}_n\}$. The objective function of the members in the population is expressed as $\vec{O} = \{O_1, O_2, \ldots, O_n\}$. According to the series of rules and strategies of the algorithm, guide and control the population in the search space, continuously update the position of each member, and dynamically evaluate new positions using an objective function. This process will gradually optimize the solution to the problem with each iteration and randomly generate the position of each member i in the search space, and the equation is as follows:

$$x_i = rand\,(1,d) * (ub - lb) + lb \tag{8}$$

   where x_i is the location of the prey, lb the minimum value (lower bound) of the problem variable, ub the maximum value (upper bound) of the problem variable, and d the number (dimension) of the problem variable.

2) Predator search strategy
   The prey is usually in groups, and hunters often choose prey that is far away from the group as their hunting target. This strategy is similar to the exploration strategy in algorithms and tends to exhibit highly random behavior. The equation for updating the hunter's position is as follows:

$$x_{i,j}\,(t+1) = x_{i,j}\,(t) + 0.5\left[\left(2CZP_{pos(j)} - x_{i,j}\,(t)\right) + \left(2\,(1-C)\,Z \cdot \gamma\,(j) - x_{i,j}\,(t)\right)\right] \tag{9}$$

   where $x_{i,j}(t)$ is the current position of the predator, $x_{i,j}(t+1)$ the updated location of the predator, P_{pos} the location of the prey, $\gamma(j)$ the average of all locations, Z an adaptive parameter, and C a balance parameter between exploration and development. The calculation equation for C, Z, and $\gamma(j)$ are as follows:

$$C = 1 - \omega\left(\frac{0.98}{\omega_{\max}}\right) \tag{10}$$

$$P = \vec{R}_1 < C \tag{11}$$

$$U = (P == 0) \tag{12}$$

$$Z = R_2 \otimes U + \vec{R}_3 \otimes (\sim U) \tag{13}$$

$$\gamma = \frac{1}{n}\sum_{i=1}^{n} \vec{x}_i \tag{14}$$

   where ω is the current number of iterations, and $\omega_{\max}$ is the maximum number of iterations. $\vec{R}_1$ and $\vec{R}_3$ are random vectors within the range of $[0, 1]$; R_2 is a random number; P is a random vector related to the number of variables; and U is the index value of the vector $\vec{R}_1$ that satisfies the condition $(P == 0)$.
   In order to solve the convergence delay caused by considering the maximum distance between members and the average position in each iteration, a decreasing mechanism is introduced, and the equation for calculating the prey position is:

$$\vec{P}_{pos} = \vec{x}_i | a\ is\ sorted\ D_{euc}\,(k_{best}), \quad k_{best} = round\,(C \times N) \tag{15}$$

   where $D_{euc}(k)$ is the Euclidean distance from the average position of each member, k_{best} a decreasing mechanism, and N the number of search agents.

3) Prey escape strategy

The safest position for prey is the global optimal position, because only in this way the prey can have a chance of survival. The equation for updating prey position is as follows:

$$x_{i,j}(t+1) = H_{pos} + C \cdot Z \cos(2\pi R_4) \times (H_{pos} - x_{i,j}(t)) \tag{16}$$

where H_{pos} is the globally optimal position, and R_4 is the random number in the range of $[-1, 1]$. The cos function locates the next prey position in the globally optimal position with different radial and angles, thus improving the performance in the development phase.

4) The choice between hunter and prey

In order to select hunter and prey, the corresponding selection mechanism is given by combining Equations (9) and (16), and the equation is as follows:

$$x_{i,j}(t+1) = \begin{cases} x_{i,j}(t) + 0.5 \left[\left(2CZP_{pos(j)} - x_{i,j}(t)\right) + (2(1-C)Z \cdot \gamma(j) - x_{i,j}(t))\right] & R_5 < \delta \quad \text{(17a)} \\ H_{pos} + C \cdot Z \cos(2\pi R_4) \times (H_{pos} - x_{\alpha,\beta}(t)) & R_5 \geq \delta \quad \text{(17b)} \end{cases}$$

where R_5 is a random number within the range of $[0, 1]$ and is an adjustment parameter.

3.2. Fuch Infinite Folding Chaos Strategy

Fuch is an infinitely collapsible chaotic map. Compared to traditional chaotic maps, Fuch maps have better ergodicity, dynamism, and convergence. Therefore, Fuch maps are selected to generate the initial population of Hunter Prey Optimization (HPO). In the algorithm, Fuch chaotic mapping values replace randomly generated values to generate the positions of hunters and prey during the initialization phase. The mathematical expression of Fuch chaotic mapping is shown in Equation (18):

$$x(t+1) = \cos\left(\frac{1}{x(t)^2}\right) \tag{18}$$

where $x(t) \neq 0$, $x \in Z^+$, $t = 1, 2, \ldots, T$.

3.3. Golden Sine Algorithm

In this paper, Golden Sine (GS) Algorithm [25] is introduced into the HPO exploration phase position update, and golden partition search is used to enable individuals in the search space to search by the optimal path, so that individuals can continuously search for the optimal solution in the search space. The algorithm can traverse all values on the sine function according to the relationship between the sine function and the unit circle thus improving the global exploration capability of the algorithm. At the same time, the golden partition coefficient enables the search individual to update the distance and direction in fixed steps and to continuously reduce the space to be explored so that the individual can search in the region of the target location (rather than the entire search space), thus improving the local exploitation capability of the algorithm. The mathematical expression of the golden sine strategy is shown in Equation (19):

$$x_i(t+1) = \begin{cases} x_i(t) \times |\sin(R_1)| + R_2\sin(R_1) \times |x_1 x_{prey}(t) - x_2 x_i(t)| & q \geq 0.5 \quad \text{(19a)} \\ [x_{prey}(t) - x_m(t)] - r_1 [lb_i + r_2(ub_i - lbi)] & q < 0.5 \quad \text{(19b)} \end{cases}$$

where $R_1 \in [0, 2\pi]$, $R_2 \in [0, \pi]$, $x_1 = -\pi\tau + \pi(1-\tau)$ and $x_2 = \pi\tau - \pi(1-\tau)$ are coefficients calculated through the golden ratio, which can make individuals search for space closer to the target value $\tau = (\sqrt{5}-1)/2$.

3.4. Principles of PMSM Parameter Identification

The identification of multiple parameters for PMSM can be actually transformed into a system optimization solution problem. The identification process of PMSM is based on the fitness function obtained from the output of the identification model and the actual value of the system. Through optimization algorithms, the parameters to be identified in the identification model are continuously

modified to identify the motor parameters. Firstly, construct a fourth order full rank PMSM parameter identification model similar to formula (4), as shown in Equation (20).

$$\begin{cases} \hat{u}_{d0}(k_0) = -\omega_{e0}(k_0)\hat{L}_q i_{q0}(k_0) \\ \hat{u}_{q0}(k_0) = \hat{R}_s i_{q0}(k_0) + \hat{\psi}_f \omega_{e0}(k_0) \\ \hat{u}_{d1}(k_1) = \hat{R}_s i_{d1}(k_1) - \hat{L}_q \omega_{e1}(k_1) i_{q1}(k_1) \\ \hat{u}_{q1}(k_1) = \hat{R}_s i_{q1}(k_1) + \hat{\psi}_f \omega_{e1}(k_1) + \hat{L}_d \omega_{e1}(k_1) i_{d1}(k_1) \end{cases} \quad (20)$$

Then the algorithm continuously filters the parameters to be identified in PMSM, minimizing the values of the identification model and fitness function. The voltage of the identification model is closer to the actual value, resulting in the parameters to be identified being closer to the actual value. The fitness function is shown in Equation (20):

$$f\left(\hat{\theta}\right) = x_1 \left|u_{d0}(k) - \hat{u}_{d0}(k)\right| + x_2 \left|u_{q0}(k) - \hat{u}_{q0}(k)\right| + x_3 \left|u_{d1}(k) - \hat{u}_{d1}(k)\right| + x_4 \left|u_{q1}(k) - \hat{u}_{q1}(k)\right| \quad (21)$$

where x_1, x_2, x_3, and x_4 are the weights, and they are all taken as 0.25, indicating that the four variables are equally important.

The principle of PMSM multi-parameter identification based on Fuch Infinite Folding Chaos-Golden Sine Algorithm (FG)-HPO is shown in Figure 2.
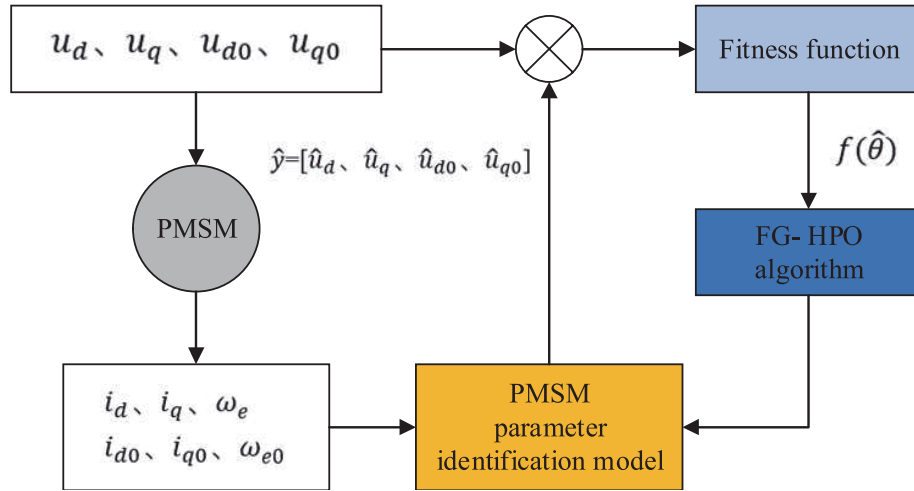

Figure 2. The schematic diagram of multi-parameter identification based on FG-HPO.

3.5. Process of FG-HPO Algorithm

In summary, the process of the FG-HPO algorithm is as follows:

Step 1: Set algorithm parameters and generate initial positions of hunters and prey through Fuch mapping.

Step 2: Use Golden Sine Algorithm (GSA) to optimize the search path of hunters and the escape path of prey.

Step 3: Update the position of hunters and prey through equations.

Step 4: Calculate fitness values and evaluate global optimal positions.

Step 5: Determine whether the maximum number of iterations has been reached. If it is reached, output the global optimal position. Otherwise, return to step 3.

3.6. Parameter Identification Based on FG-HPO Algorithm and Dead-time Compensation

The simulation block diagram of PMSM parameter identification based on FG-HPO algorithm under vector control is shown in Figure 3.
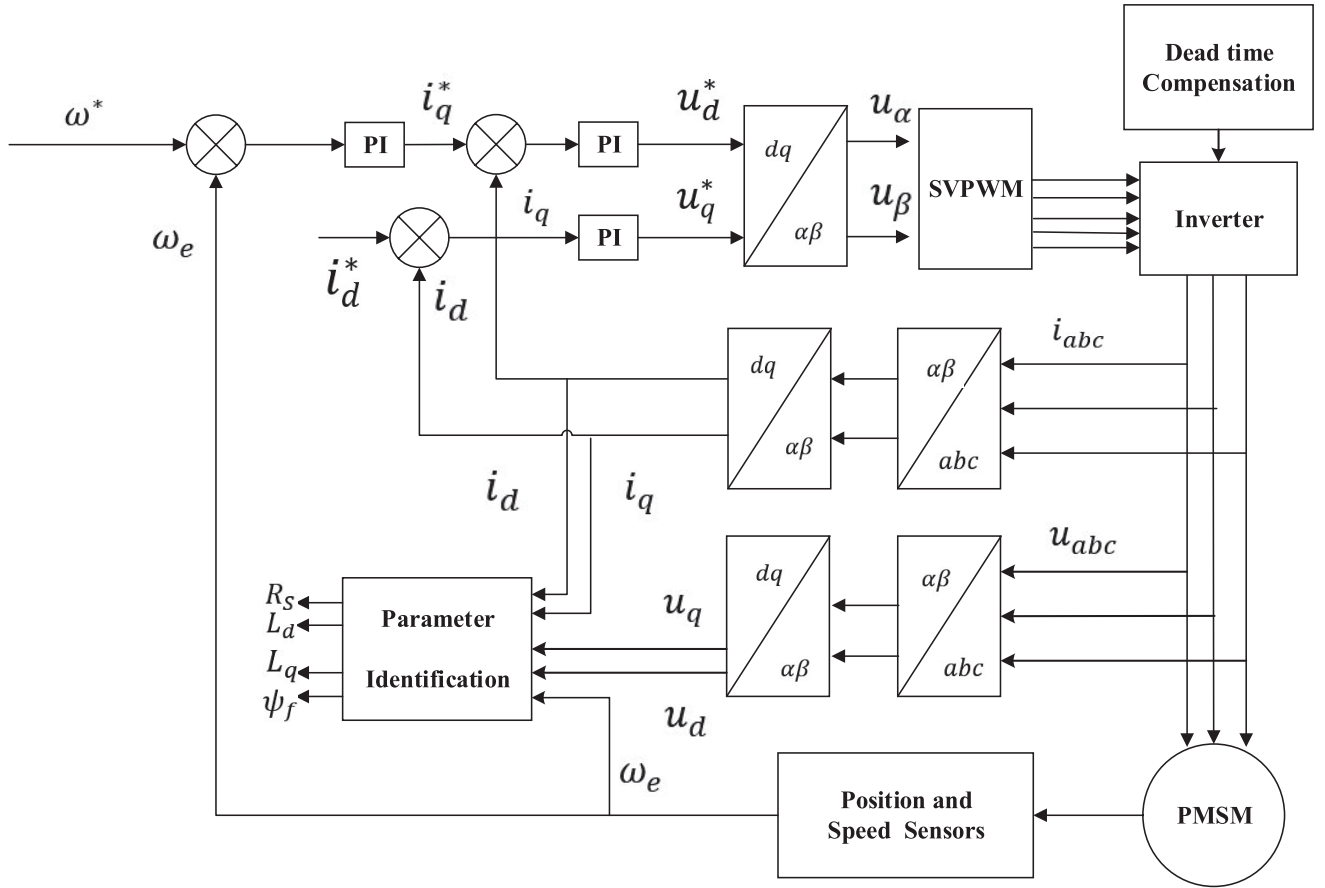
Figure 3. The simulation block diagram of PMSM parameter identification based on FG-HPO algorithm under vector control.

4. SIMULATION AND EXPERIMENTAL VERIFICATION

4.1. Algorithm Performance Test

In order to prove the superiority of the improved algorithm, five standard test functions are selected for testing and compared with HPO algorithm, Particle Swarm Optimization (PSO) algorithm, Sparrow Search algorithm (SSA), and Whale Optimization Algorithm (WOA). The first three functions are unimodal functions, and the last two functions are multimodal functions. The standard test function information is shown in Table 1, where Dim represents the dimensions of the function; Range is the boundary of the function's search space; and Fmin is the optimal value. The results of algorithm optimization and comparison experiments are shown in Table 2.

4.2. Simulation Results and Analysis

In order to verify the improvement effect of dead time compensation and the parameter identification performance based on FG-HPO algorithm, a PMSM vector control simulation model is established in MATLAB/SIMULINK environment. The motor parameters used are shown in Table 3.

The phase current waveform under vector control is shown in Figure 4, and the fast Fourier transform (FFT) analysis diagram of phase current is shown in Figure 5 (Taking A-phase current as an example).

According to motor vector control simulation experiments, the A-phase current waveforms before and after adding dead time compensation were compared. The results show that after adding dead

Table 1. Standard test function.

Num	Function	Dim	Range	Fmin
1	$F_1(x) = \sum_{i=1}^{n} \left(\sum_{j=1}^{i} x_j \right)^2$	30	$[-100, 100]$	
2	$F_2(x) = \max\{|x_i|, 1 \le i \le n\}$	30	$[-100, 100]$	0
3	$F_3(x) = \sum_{i=1}^{n} \left[100\left(x_{i+1} - x_i^2\right)^2 + (x_i - 1)^2 \right]$	30	$[-30, 30]$	
4	$F_4(x) = -20\exp\left(-0.2\sqrt{\frac{1}{n}\sum_{i=1}^{n} x_i^2}\right)$ $- \exp\left(\frac{1}{n}\sum_{i=1}^{n}\cos(2\pi x_i)\right) + 20 + e$	30	$[-32, 32]$	
5	$F_5(x) = \frac{1}{4000}\sum_{i=1}^{n} x_i^2 - \prod_{i=1}^{n}\cos\left(\frac{x_i}{\sqrt{i}}\right) + 1$	30	$[-600, 600]$	0

Table 2. The results of algorithm optimization and comparison experiments.

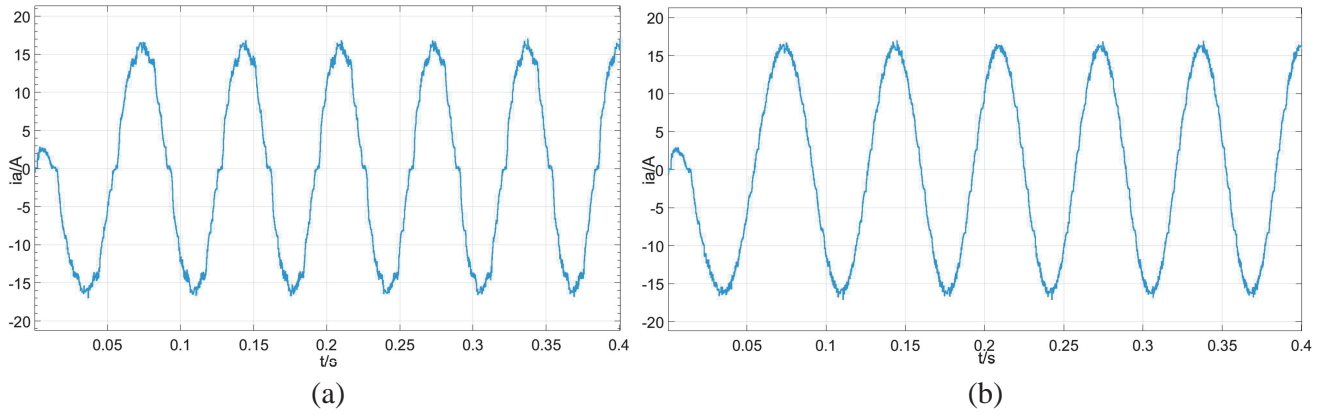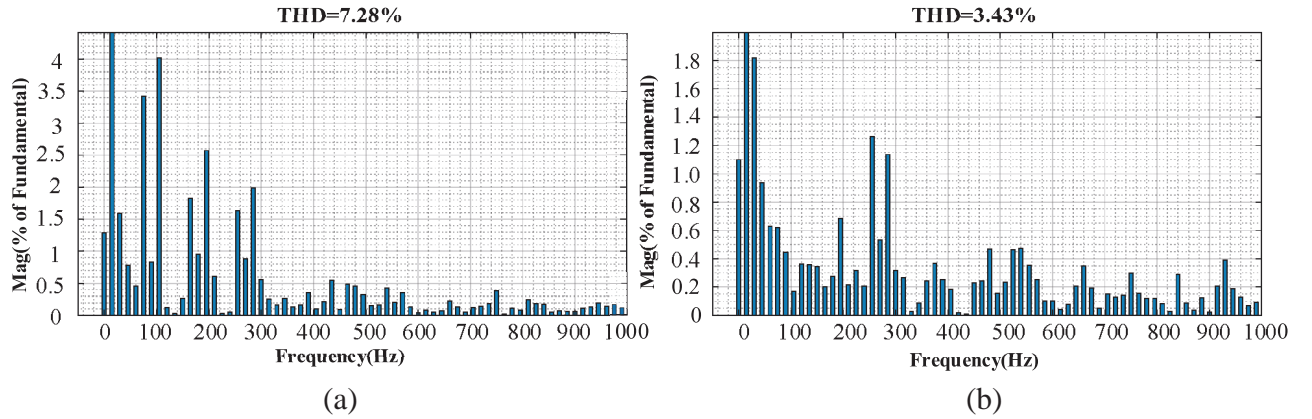| Function		FG-HPO	HPO	PSO	SSA	WOA
F_1	worst	6.15e-125	516e-06	3435.4234	43517e-73	99538.151
	best	8.156e-159	4.151e-1	2761562	84316e-107	46262.251
	avg	10.364e-146	1.121e-03	6604908	6.1521e-81	65656.8815
	std	4.22e-145	0.0056217	4305412	6.151e-51	234654611
F_2	worst	3.1568e-79	3.1565	11652	3.1205e-51	76.1561
	best	6.6132e-84	0.9153	41564	1.1615e-66	3.1566
	avg	3.498e-80	0.69541	6.1515	6.1563e-52	46.1597
	std	9.1521e-81	0.4365	1.2165	1.1516e-51	34.15169
F_3	worst	27.0137	21.1536	33494693	1.15e-03	316641
	best	21.1664	17.1651	66.256	8725e-05	241326
	avg	24.1517	194056	1676039	2162e-04	291513
	std	0.3212	0.8826	621.752	0.013516	0.61396
F_4	worst	8.8818e-16	8.8818e-16	1.8e-4	3.1511	8.8818e-16
	best	8.8818e-16	8.8818e-16	4.1532	17.1561	8.8818e-16
	avg	8.8818e-16	8.8818e-16	6.1536	8.156	8.8818e-16
	std	0	0	1.5621	4.216	0
F_5	worst	0	0	5.4151e-08	0	0
	best	0	0	1511e-03	0	0
	avg	0	0	165e-05	0	0
	std	0	0	0.651	0	0

time compensation, the total harmonic distortion (THD) of phase current is reduced from 7.28% to 3.43% through FFT analysis. The content of current fundamental wave is increased, and the content of high-order harmonics is significantly reduced. This method is proved to effectively improve the current waveform and eliminate zero current clamping phenomenon.

The results and errors of each identification algorithm are shown in Table 4.

From Table 4, it can be seen that basic algorithms without optimization are prone to falling into local optima, resulting in significant accuracy errors. After calculation, the maximum error rates for parameter identification of d-axis inductance and q-axis inductance are 7.81% and 7.86%, respectively. The maximum error rate for flux identification is 6.41%, and the maximum error rate for stator

Table 3. Main parameters of the motor.

parameter	numerical value
sampling period/s	10e-6
stator resistance/Ω	0.958
Q axis inductance L_q/mH	12
D axis inductance L_d/mH	12
flux linkage ψ_f/Wb	0.1827
number of pole pairs P_n	4
Rotational inertia J/$(\mathrm{kg} \cdot \mathrm{m}^2)$	0.003

(a)   (b)

Figure 4. The diagram of A-phase current at a speed of 600 r/min. (a) Without dead time compensation. (b) With dead time compensation.

(a)   (b)

Figure 5. The FFT analysis diagram of A-phase current at a speed of 600 r/min. (a) Without dead time compensation. (b) With dead time compensation.
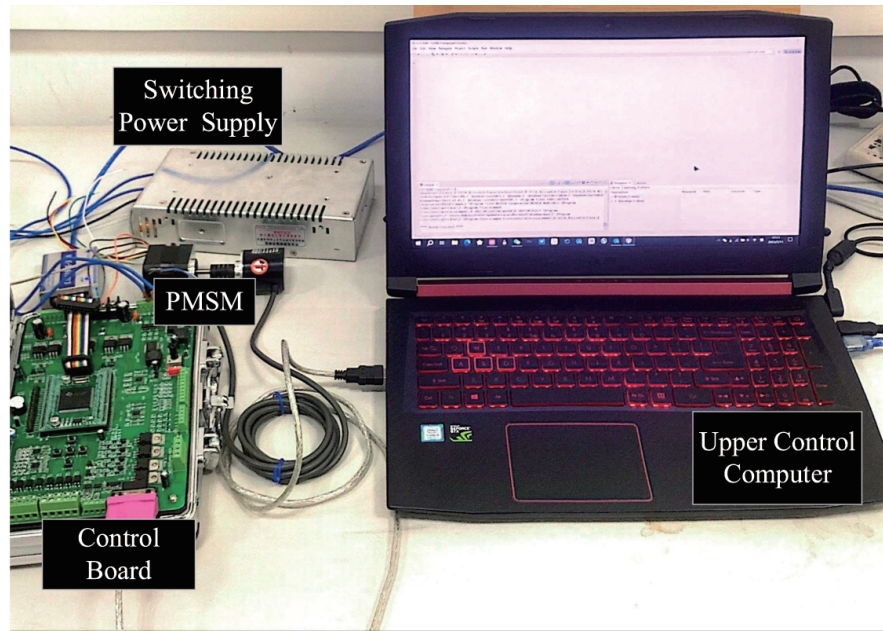
resistance identification is 6.94%. In comparison, the error rates for magnetic flux identification of d-axis inductance and q-axis inductance based on the FG-HPO algorithm are 2.13% and 2.06%, respectively. The identification error rates for magnetic linkage are 2.23%, and the identification error rates for stator resistance are 1.92%. It shows that the improved HPO algorithm has higher recognition accuracy, faster Rate of convergence, and better jump out of the local optimal solution than other algorithms.

Table 4. The results and errors of each identification algorithm.

Parameter	FG-HPO	HPO	PSO	HHO	WOA
Stator d-axis inductance/mH	11.744	11.677	11.0628	11.266	11.425
Error/%	2.13	2.69	7.81	6.12	4.79
Stator q-axis inductance/mH	11.753	11.72	11.141	11.2488	11.501
Error/%	2.06	2.33	7.16	6.26	4.16
Permanent magnet flux linkage/Wb	0.179	0.178	0.171	0.173	0.175
Error/%	2.03	2.6	6.41	5.3	4.2
Motor stator resistance/Ω	0.94	0.932	0.892	0.92	0.919
Error/%	1.88	2.71	6.99	3.9	4.1

4.3. Experimental Results and Analysis

In order to further verify the effectiveness of the improved algorithm, a PMSM vector control platform is built, as shown in Figure 6. The experimental platform adopts a control system with DSP28305 as the core, a 24 V switching power supply, and a PMSM. The motor parameters are shown in Table 3. After the motor runs stably, the method shown in Figure 1 is used to sample the motor parameters to complete parameter identification.

Figure 6. The experimental platform.

By conducting vector control experiments on the platform shown in Figure 6, the results of parameter identification are shown in Figure 7.

It can be observed from Figure 6 that the steady-state error of the identification algorithm decreases after the dead time is compensated. The identification error of stator resistance decreases from 4.23% to 2.03%; the identification error of magnetic linkage decreases from 3.57% to 1.93%; the identification error of d-axis inductance decreases from 2.87% to 2.21%; and the identification error of q-axis inductance decreases from 3.48% to 2.01%. Thus, the effect of adding dead time compensation on improving parameter identification is better verified.
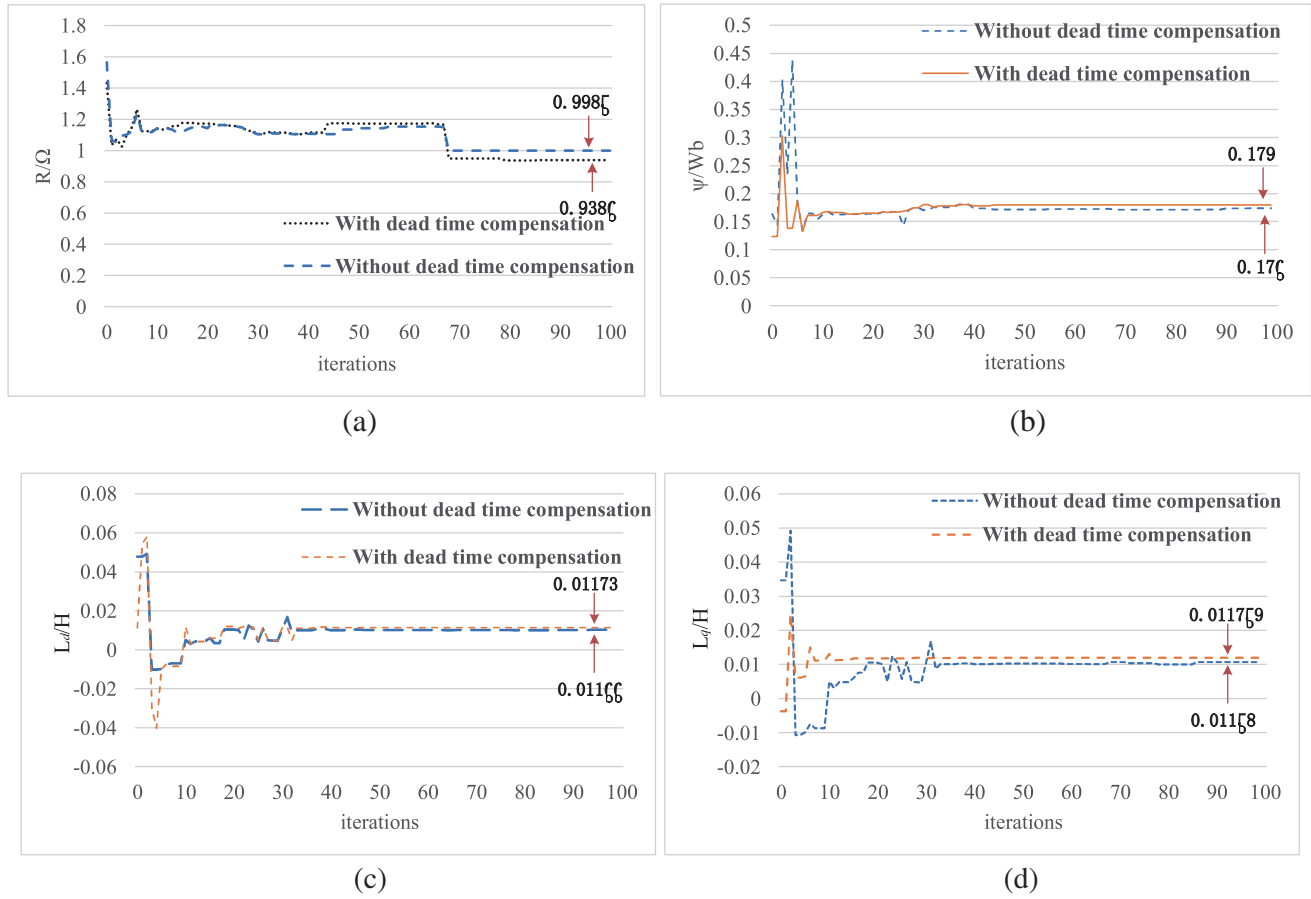
(a)

(b)

(c)

(d)

Figure 7. Results of parameter identification. (a) Identification results of stator resistance. (b) Identification results of magnetic linkage. (c) Identification results of d-axis inductance. (d) Identification results of q-axis inductance.

5. CONCLUSION

The research content and results of this article are summarized as follows:

An ideal PMSM mathematical model is established and analyzed. The underrank problem of PMSM parameter identification equations is solved by injecting negative sequence current under vector control method.

For the dead time effect of voltage source inverters, a rotating coordinate compensation method is used to compensate the dead time voltage. Simulation experiments show that it can effectively reduce current harmonics and suppress zero current clamping effect.

The HPO algorithm has been optimized and improved, and the superiority of FG-HPO has been verified by comparing it with other basic algorithms through standard function testing. The comparison results in motor parameter identification simulation show that the improved HPO algorithm has higher accuracy and faster speed.

The PMSM vector control experimental platform is built. By comparing the motor parameter identification results before and after adding dead time compensation, it is of great necessity to add dead time compensation to improve the accuracy of parameter identification.

REFERENCES

1. Rafaq, M. S. and J. Jung, "A comprehensive review of state-of-the-art parameter estimation techniques for permanent magnet synchronous motors in wide speed range," *IEEE Transactions on Industrial Informatics*, Vol. 16, No. 7, 4747–4758, 2020.

2. Ni, R., D. Xu, G. Wang, et al., "Maximum efficiency per ampere control of permanent-magnet synchronous machines," *IEEE Transactions on Industrial Electronics*, Vol. 62, No. 4, 2135–2143, 2015.

3. Zhu, Z. Q., D. Liang, and K. Liu, "Online parameter estimation for permanent magnet synchronous machines: An overview," *IEEE Access*, Vol. 9, 59059–59084, 2021.

4. Sandre-Hernandez, O., R. Morales-Caporal, J. Rangel-Magdaleno, et al., "Parameter identification of PMSMs using experimental measurements and a PSO algorithm," *IEEE Transactions on Instrumentation and Measurement*, Vol. 64, No. 8, 2146–2154, 2015.

5. Huang, Y., T. Tao, Y. Liu, K. Chen, and F. Yang, "DSC-FLL based sensorless control for permanent magnet synchronous motor," *Progress In Electromagnetics Research M*, Vol. 98, 171–181, 2020.

6. Zhang, Y., Z. Ming, and Z. Cheng, "Parameter identification of PMSWG Based on ASMDRPSO," *Progress In Electromagnetics Research C*, Vol. 126, 253–265, 2022.

7. Wang, T., J. Huang, M. Ye, et al., "An EMF observer for PMSM sensorless drives adaptive to stator resistance and rotor flux linkage," *IEEE Journal of Emerging and Selected Topics in Power Electronics*, Vol. 7, No. 3, 1899–1913, 2019.

8. Cheng, Y., M. Y Zhao, and Q. Liu, "Online parameter identification of PMSM based on LAWPSO," *2020 IEEE 4th Infor. Tech., Networking, Electronic and Automation Control Conference (ITNEC)*, 2188–2192, 2020.

9. Liu, K. and Z. Q. Zhu, "Position offset-based parameter estimation for permanent magnet synchronous machines under variable speed control," *IEEE Transactions on Power Electronics*, Vol. 30, No. 6, 3438–3446, 2015.

10. Dang, D. Q., M. S. Rafaq, H. H. Choi, et al., "Online parameter estimation technique for adaptive control applications of interior PM synchronous motor drives," *IEEE Transactions on Industrial Electronics*, Vol. 63, No. 3, 1438–1449, 2016.

11. Chen, J. and J. Huang, "Stable simultaneous stator and rotor resistances identification for speed sensorless induction motor drives: Review and new results," *IEEE Transactions on Power Electronics*, Vol. 33, No. 10, 8695–8709, 2018.

12. Chen, J. and J. Huang, "Online decoupled stator and rotor resistances adaptation for speed sensorless induction motor drivers by a time-division approach," *IEEE Transactions on Power Electronics*, Vol. 32, No. 6, 4587–4599, 2017.

13. Chen, J., J. Huang, and Y. Sun, "Resistances and speed estimation in sensorless induction motor drives using a model with known regressors," *IEEE Transactions on Industrial Electronics*, Vol. 66, No. 64, 2659–2667, 2019.

14. Chen, J. and J. Huang, "Globally stable speed-adaptive observer with auxiliary states for sensorless induction motor drives," *IEEE Transactions on Power Electronics*, Vol. 34, No. 1, 33–39, 2019.

15. Wang, T., J. Huang, M. Ye, et al., "An EMF observer for PMSM sensorless drives adaptive to stator resistance and rotor flux linkage," *IEEE Journal of Emerging and Selected Topics in Power Electronics*, Vol. 7, No. 3, 1899–1913, 2019.

16. Deng, W., C. Xia, Y. Yan, et al., "Online multi-parameter identification of surface-mounted PMSM considering inverter disturbance voltage," *IEEE Transactions on Energy Conversion*, Vol. 32, No. 1, 202–212, 2017.

17. Wu, C., Y. Zhao, and M. Sun, "Enhancing low-speed sensorless control of PMSM using phase voltage measurements and online multiple parameter identification," *IEEE Transactions on Power Electronics*, Vol. 35, No. 10, 10700–10710, 2020.

18. Liu, Z., H. Wei, Q. Zhong, et al., "GPU implementation of DPSO-RE algorithm for parameters identification of surface PMSM considering VSI nonlinearity," *IEEE Journal of Emerging and Selected Topics in Power Electronics*, Vol. 5, No. 3, 1334–1345, 2017.

19. Li, X. and R. Kennel, "General equationtion of kalman-filter-based online parameter identification methods for VSI-fed PMSM," *IEEE Transactions on Industrial Electronics*, Vol. 68, No. 4, 2856–2864, 2021.

20. Liu, Z., H. Wei, X. Li, et al., "Global identification of electrical and mechanical parameters in PMSM drive based on dynamic self-learning PSO," *IEEE Transactions on Power Electronics*, Vol. 33, No. 12, 10858–10871, 2018.

21. Liu, X., Y. Pan, L. Wang, J. Xu, Y. Zhu, Z. Li, et al., "Model predictive control of permanent magnet synchronous motor based on parameter identification and dead time compensation," *Progress In Electromagnetics Research C*, Vol. 120, 253–263, 2022.

22. Kim, H.-S., K.-H. Kim, and M.-J. Youn, "On-line dead-time compensation method based on time delay control," *IEEE Transactions on Control Systems Technology,* Vol. 11, No. 2, 279–285, 2003.

23. Morimoto, S., A. Shimmei, M. Sanada, and Y. Takeda, "Position and speed sensorless control system of permanent magnet synchronous motor with parameter identification," *Electrical Engineering in Japan*, Vol. 160, No. 2, 68–76, 2007.

24. Naruei, I., F. Keynia, and A. Sabbagh Molahosseini, "Hunter-prey optimization: Algorithm and applications," *Soft Computing*, Vol. 26, 1279–1314, 2022.

25. Tanyildizi, E. and G. Demir, "Golden sine algorithm: A novel math-inspired algorithm," *Advances in Electrical and Computer Engineering*, Vol. 17, No. 2, 71–78, 2017.